Forkhead box O1 (FOXO1) is an important tumor suppressor that regulates several cellular processes, including apoptosis induction, cell cycle arrest, and DNA repair [4]. In cancer cells, FOXO1 downregulation is associated with cancer progression and resistance to chemotherapy [5–7], and its function is inhibited by the phosphatidylinositol 3-kinase–Akt–FOXO1 axis [8]. Therefore, the FOXO1 regulating mechanism has been speculated to be a promising target to overcome refractory GC.

Protein arginine methyltransferases (PRMTs) are enzymes that catalyze the transfer of a methyl group from *S*-adenosylmethionine to arginine [9]. Arginine methylation plays many important roles in cellular processes, including RNA processing, transcriptional regulation, and protein–protein interactions [9]. PRMT1 is a predominant methyltransferase with a wide substrate spectrum, including FOXO1 and BCL-2 antagonist of cell death (BAD) [10] [11]. The tumor suppressor FOXO1 and the apoptosis-related gene BAD are activated and translocated in the nucleus via arginine methylation by PRMT1. Conversely, phosphatidylinositol 3-kinase-Akt signaling suppresses the function and nuclear translocation of FOXO1 and BAD.

In several cancers, PRMT1 overexpression is related to disease progression and prognosis [12–14]. Moreover, some studies reported that PRMT1 was associated with the inhibition of proliferation and apoptosis induction in lung cancer and gliomas [15, 16]. On the other hand, PRMT1 inhibition was reported to induce suppression of the proliferation potency of bladder and lung cancer cells [17] and enhanced chemosensitivity via inhibition of DNA repair in osteosarcoma cells [18]. These data suggested that PRMT1 plays various important roles in several types of cancer cells. However, few studies have addressed the clinical significance of PRMT1 expression in GC.

The aim of this study was to evaluate expression levels and identify correlations between PRMT1 and FOXO1 to determine whether expression levels of these genes can be used as markers of prognosis and chemosensitivity in GC. Moreover, we performed PRMT1 suppression analysis to clarify the relationship between PRMT1 and chemosensitivity using GC cell lines.

Materials and methods

Clinical samples and cell lines

Surgical specimens were obtained from 195 GC patients (137 men and 58 women) who underwent potentially curative surgery in the Department of General Surgical Science, Gunma University, between 1999 and 2006. All patients provided written informed consent before participation in this study. The mean patient age was 64.9 years (range 29–88 years). 5-Fluorouracil (5-FU)-based adjuvant chemotherapy was administered to 80 GC patients. The pathological characteristics of the specimens were classified on the basis of the 14th edition of the Japanese Classification of Gastric Carcinoma outlined by the Japanese Gastric Cancer Association. None of the patients received irradiation or chemotherapy before surgery.

The human GC cell lines MKN7, MKN45, MKN74, KATOIII, and AZ521 were provided by the JCRB Cell Bank and RIKEN Cell Bank. All cells were cultured in Roswell Park Memorial Institute 1640 medium supplemented with penicillin at 100 U/mL, streptomycin at 100 U/mL, and 10 % fetal bovine serum in a humidified atmosphere of 5 % CO_2 at 37 °C.

Tissue microarrays

Formalin-fixed, paraffin-embedded clinical samples were stored in the archives of the Clinical Department of Pathology, Gunma University Hospital. For each patient, one paraffin block containing representative nonnecrotic tumor areas was selected. GC tissue cores (2.0-mm diameter per tumor) were punched out from the representative areas near the invasive front and transferred into the paired recipient paraffin block by means of a tissue array instrument (Beecher Instruments, Silver Spring, MD, USA).

Immunohistochemical analysis

Tissue sections (2 μm thick) were subjected to immunohistochemical staining. In brief, all sections were incubated at 60 °C for 60 min and deparaffinized in xylene, rehydrated, and incubated with fresh 0.3 % hydrogen peroxide in 100 % methanol for 30 min at room temperature to block endogenous peroxidase activity. After rehydration by means of a graded series of ethanol, antigen retrieval was performed with the ImmunoSaver antigen retriever system (Electron Microscopic Sciences, Hattsfield, PA, USA) at 98–100 °C for 30 min, and sections were subsequently passively cooled to room temperature. After the sections had been rinsed in 0.1 M phosphate-buffered saline (pH 7.4), nonspecific binding sites were blocked by incubation with protein block serum-free reagent (Dako, Carpinteria, CA, USA) for 30 min. The sections were then incubated with rabbit anti-PRMT1 monoclonal antibody (OriGene Technologies, Rockville, MD, USA) and rabbit anti-FOXO1 monoclonal antibody (Cell Signaling Technology, Danvers, MA, USA) at a dilution of 1:200 overnight at 4 °C and at room temperature for 30 min, respectively. The reactions were visualized with a Histofine Simple Stain MAX PO (Multi) kit (Nichirei Biosciences, Tokyo, Japan) according to the manufacturer's instructions. The chromogen 3,3′-diaminobenzidine tetrahydrochloride was

applied as a 0.02 % solution in 50 mM ammonium acetate–citric acid buffer (pH 6.0) containing 0.005 % hydrogen peroxide. The sections were lightly counterstained with hematoxylin and mounted. No detectable staining of negative controls incubated without the primary antibody was evident.

Evaluation of immunostaining

Immunohistochemistry slides were scanned and evaluated by two experienced examiners. The intensity of nuclear PRMT1 and FOXO1 was scored as follows: 0 for no staining; 1+ for weak staining; 2+ for moderate staining; and 3+ for strong staining. Nuclear immunoreactivity of PRMT1 was assessed as follows: (1) a low expression group, i.e., no staining, cytoplasmic staining, weak nuclear staining, or moderate nuclear staining of tumor cells, defined as scores of 0, 1+, and 2+; and (2) a high expression group, i.e., strong nuclear staining of tumor cells, defined as a score of 3+. Nuclear immunoreactivity of FOXO1 was assessed as follows: (1) a low expression group, i.e., no staining and cytoplasmic staining of tumor cells, defined as a score of 0; and (2) a high expression group, i.e., weak nuclear staining, moderate nuclear staining, or strong nuclear staining of tumor cells, defined as scores of 1+, 2+, and 3+.

RNA interference of PRMT1 expression

PRMT1-specific small interfering RNA (siRNA) 1 (sense sequence, GUGAGAAGCCCAACGCUGAtt), PRMT1-specific siRNA2 (sense sequence, CCGUCAAGGUGGA AGACCUtt), and a negative control siRNA were purchased from Bonac (Kurume, Japan). MKN7 GC cells were seeded at 2×10^5 cells per well in a volume of 2 mL in six-well flat-bottom plates and incubated in a humidified atmosphere of 5 % CO_2 at 37 °C. After 24 h of incubation, the siRNAs were mixed with 200 μL of Opti-MEM™ medium (Life Technologies, Carlsbad, CA, USA) and 4 μL of Lipofectamine RNAiMAX (Life Technologies), and incubated for 20 min. Next, the reagents and 800 μL of Opti-MEM were added to each well. RNA interference assays were performed after a 48-h incubation period.

Protein extraction and Western blot analysis

Western blot analysis was used to confirm the expression of PRMT1, FOXO1, and β-actin in the GC cell lines. Total proteins were extracted with PROPREP protein extraction solution (iNtRON Biotechnology, Seongnam, South Korea). Nuclear proteins were extracted with a LysoPure™ nuclear and cytoplasmic extractor kit (Wako Pure Chemical Industries, Osaka, Japan). These proteins were electrophoresed through NuPAGE 4–12 % [bis(2-hydroxyethyl)amino]tris(hydroxymethyl)methane gels (Life Technologies) and then electrotransferred to poly(vinylidene difluoride) membranes. The membranes were blocked with 5 % skim milk or 5 % bovine serum albumin, and the proteins were detected with use of an anti-PRMT1 antibody (dilution, 1:1000; OriGene Technologies), an anti-FOXO1 antibody (dilution, 1:1000; Cell Signaling Technology), an anti-phosphorylated FOXO1 (p-FOXO1) antibody (dilution, 1:1000; Abcam, Cambridge, UK), and an anti-phosphorylated BAD (p-BAD) antibody (dilution, 1:1000; Abcam), with anti-β-actin antibody (dilution, 1:1000; Sigma-Aldrich, St Louis, MO, USA) and anti-histone deacetylase 1 antibody (dilution, 1:1000; Santa Cruz Biotechnology, Santa Cruz, CA, USA) serving as controls. Bands were stained with ECL Prime Western blotting detection reagent, and band intensities were calculated with an Image Quant LAS 4000 digital imaging system (GE Healthcare Life Sciences, Cleveland, OH, USA).

Chemosensitivity analysis

MKN7 and MKN45 cells transfected with PRMT1 siRNAs were dispensed into 96-well plates. Twenty-four hour after the initial seeding, cisplatin and 5-FU were added for 48 h (cisplatin final concentrations of 0, 1.0, 2.0, 4.0, 8.0, and 16 μg/mL; 5-FU final concentrations of 0, 0.1, 1.0, 10, 100, and 1000 μg/mL). To quantitate cell viability with the water-soluble tetrazolium salt WST-8 assay (Dojindo Molecular Technologies, Rockville, MD, USA), 10 μL of the cell counting solution was added to each well, and the plates were incubated at 37 °C for 2 h. We determined cell viability by measuring the absorbance of the medium at 450 nm, with the reference wavelength set at 650 nm. The absorbance values were read with an xMark microplate absorbance spectrophotometer (Bio-Rad Laboratories, Hercules, CA, USA).

Statistical analysis

For continuous variables, the data are expressed as the mean ± standard deviation. The relationship between PRMT1 expression and the clinicopathological factors and in vitro assay data were analyzed by Student's *t* test, the chi-square test, and analysis of variance. Overall survival curves measured from the day of surgery were plotted according to the Kaplan–Meier method, and the log-rank test was applied for comparison. A probability (*P*) value of less than 0.05 was considered statistically significant. The relative multivariate significance of potential prognostic variables was investigated. Cox proportional hazards regression analysis was used to test the independent prognostic contribution of nuclear PRMT1 expression. All

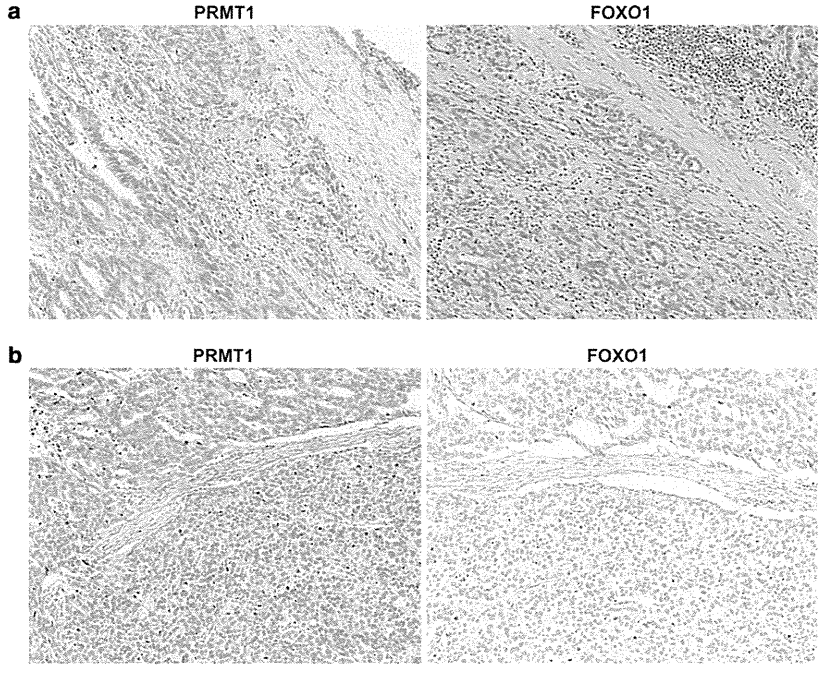

Fig. 1 Immunohistochemical analysis of protein arginine methyltransferase 1 (*PRMT1*) and forkhead box O1 (*FOXO1*) expression in representative gastric cancer tissue samples. **a** Nuclear FOXO1 (*right*) expression levels were enhanced in tissues that displayed high levels of nuclear PRMT1 expression (*left*). **b** Nuclear FOXO1 (*right*) expression levels were decreased in tissues that displayed low levels of nuclear PRMT1 expression (*left*). Magnification ×100

statistical analyses were performed with JMP (SAS Institute, Cary, NC, USA).

Results

Immunohistochemical staining of PRMT1 and FOXO1 in GC tissues

Immunohistochemical analysis showed that PRMT1 and FOXO1 expression was present in 195 GC samples. PRMT1 and FOXO1 were predominantly expressed in the nucleus. Sixty-four GC specimens (32.8 %) were assigned to the high PRMT1 expression group and 131 GC specimens (67.2 %) were assigned to the low PRMT1 expression group, whereas 131 GC specimens (67.2 %) were assigned to the high FOXO1 expression group and 64 GC specimens (32.8 %) were assigned to the low FOXO1 expression group. Our analysis revealed that nuclear FOXO1 expression was correlated with PRMT1 levels, i.e., the high PRMT1 expression group demonstrated higher FOXO1 levels than the low PRMT1 expression group (Fig. 1).

Association between the nuclear expression of PRMT1 and FOXO1 and clinicopathological factors in 195 GC samples

Correlations between PRMT1 expression and patient clinicopathological characteristics (age, sex, histological subtype, tumor depth, lymph node metastasis, lymphatic invasion, venous invasion, pathological stage, and recurrence after adjuvant chemotherapy) and FOXO1 nuclear expression levels are shown in Table 1. The results indicated that patients with low versus high tumor PRMT1 expression differed with respect to nuclear FOXO1 expression and recurrence: the low expression group had decreased FOXO1 nuclear accumulation ($P = 0.0012$) and higher recurrence

Table 1 Correlations between protein arginine methyltransferase 1 (*PRMT1*) nuclear expression and forkhead box O1 (*FOXO1*) nuclear expression and clinicopathological factors in 195 gastric cancer patients

Factors	PRMT1 nuclear expression		*P*
	Low expression ($n = 131$)	High expression ($n = 64$)	
Age (years)			
<66	67	27	0.24
≥66	64	37	
Sex			
Male	95	42	0.32
Female	36	22	
Histological subtype			
Tub	49	29	0.38
Por, Sig	76	34	
Pap, Muc	6	1	
Depth			
m, sm, mp	30	21	0.14
ss, se, si	101	43	
Lymph node metastasis			
Absent	43	18	0.51
Present	88	46	
Lymphatic invasion			
Absent	9	7	0.33
Present	122	57	
Venous invasion			
Absent	40	18	0.73
Present	91	46	
Stage			
I, II	61	33	0.51
III, IV	70	31	
FOXO1 nuclear expression			
Low	53	11	0.0012*
High	78	53	
Recurrence after adjuvant chemotherapy ($n = 80$)			
Absent	17	15	0.043*
Present	36	12	

m mucosa, *mp* muscularis propria, *Muc* mucinous adenocarcinoma, *Pap* papillary adenocarcinoma, *Por* poorly differentiated adenocarcinoma, *se* serosa, *si* adjacent structures, *Sig* signet ring cell carcinoma, *sm* submucosa, *ss* subserosa, *Tub* tubular adenocarcinoma

* $P < 0.05$

after adjuvant chemotherapy ($P = 0.043$). However, no significant differences were observed with respect to age, sex, histological subtype, tumor depth, lymph node metastasis, lymphatic invasion, venous invasion, or pathological stage.

Prognostic significance of PRMT1 expression in GC patients

Cancer-specific survival of GC patients with low PRMT1 expression tumors was significantly less favorable than that of patients with high PRMT1 expression tumors ($P = 0.04$; Fig. 2). Multivariate analysis indicated that low PROX1 expression in GC tissues was an independent prognostic marker of poor survival, similar to tumor depth, lymph node metastasis, and venous invasion ($P = 0.037$; Table 2). These results were consistent with cancer-specific survival rates of GC patients with low FOXO1 nuclear expression in tumors, which were significantly lower than those of patients with high FOXO1 expression ($P = 0.0002$; Fig. S1). On the other hand, low PRMT1 tumor expression in GC patients was not significantly associated with shorter overall survival and disease-

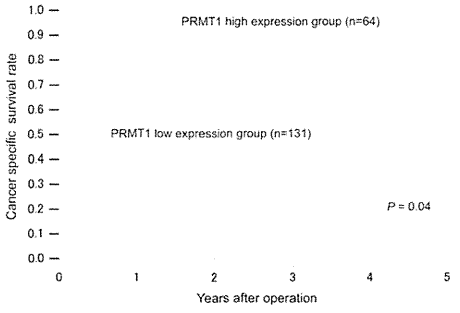

Fig. 2 Low expression levels of protein arginine methyltransferase 1 (*PRMT1*) in gastric cancer are associated with poor prognosis. Kaplan–Meier cancer-specific survival *curves* of gastric cancer patients according to the level of PRMT1 expression for the high PRMT1 expression group ($n = 64$) and the low PRMT1 expression group ($n = 131$) ($P = 0.04$)

free survival compared with those of patients with high levels of PRMT1 expression (Fig. S2a, b). However, overall survival and cancer-specific survival of GC patients with tumors with low PRMT1 expression levels treated with adjuvant therapy ($n = 80$) were worse than those with high PRMT1 expression levels ($P = 0.04$, $P = 0.037$; Fig. S2c, d).

PRMT1-specific siRNAs inhibited chemosensitivity in vitro

PRMT1 expression was detected in MKN7, KATOIII, MKN45, and AZ521 cells (Fig. 3a), whereas FOXO1 was expressed in MKN7, MKN45, and AZ521 cells. We chose two PRMT1-specific siRNAs (siRNA1 and siRNA2) to investigate how the inhibition of PRMT1 expression affected sensitivity to cisplatin and 5-FU in MKN7 and MKN45 cells. PRMT1 siRNA significantly reduced the expression levels of PRMT1 and induced nuclear expression of p-FOXO1 and p-BAD, as compared with the control siRNAs (Fig. 3b, c). The reduction in PRMT1 expression significantly inhibited sensitivity to cisplatin and 5-FU (Fig. 4).

Discussion

The results of this study demonstrate that low nuclear expression of PRMT1 was correlated with nuclear FOXO1 accumulation and recurrence after adjuvant chemotherapy and that nuclear PRMT1 expression was an independent prognostic factor for GC. These results are supported by in vitro findings showing that PRMT1 regulates GC cell chemosensitivity.

From the data in the present report and previous reports, PRMT1 is known to have a dual function as a tumor suppressor and promoter [15, 17, 19]. PRMT1 suppression may both induce antitumor effects and proliferation depending on the cell type. Three types of arginine methylation have been reported; monomethylarginine (MMA), asymmetric dimethylarginine (ADMA), and symmetric dimethylarginine (SDMA), with PRMT1 accounting for more than 90 % of the AMDA type of methylation [20]. The loss of PRMT1 increased the levels of MMA and SDMA, and PRMT1 is transported between the nucleus and cytoplasm depending on the methylation status of substrate proteins in several cells [21]. On the other hand, PRTM1 has some splicing variants, and the noncoding variant of PRMT1, PRMT1 variant 2, was reported to be associated with progression of both colon and breast cancer [13, 22]. Moreover, it was reported that PRMT1 functions such as substrate recognition and methylation are inhibited by phosphorylation of Tyr291 [23]. The disparity in PRMT1 functional analysis data may be due to the cell-specific balance of substrate methylation status, PRMT1-splicing variants, and PRMT1-phosphorylation status in each cancer cell line.

Table 2 Results of univariate and multivariate analyses of clinicopathological factors affecting the survival rate in 195 gastric cancer patients following surgery

Clinicopathological variable	Univariate analysis			Multivariate analysis		
	RR	95 % CI	*P*	RR	95 % CI	*P*
Age (<66 years/≥66 years)	1.06	0.85–1.31	0.59	–	–	–
Sex (male/ female)	0.85	0.65–1.08	0.19	–	–	–
Depth (m, sm, mp/ss, se, si)	4.89	2.42–11.69	<0.0001*	3.24	1.54–7.93	0.0011*
Lymph node metastasis (negative/ positive)	1.67	1.27–2.27	0.0001*	1.39	1.02–1.97	0.035*
Lymphatic invasion (negative/ positive)	1.74	1.06–3.51	0.024*	1.11	0.61–2.35	0.74*
Venous invasion (negative/ positive)	1.62	1.23–2.21	0.0003*	1.39	1.05–1.92	0.02*
PRMT1 expression (low/ high)	0.6	0.34–0.98	0.04*	0.59	0.34–0.97	0.037*

CI confidence interval, *m* mucosa, *mp* muscularis propria, *PRMT1* protein arginine methyltransferase 1, *RR* relative risk, *se* serosa, *si* adjacent structures, *sm* submucosa, *ss* subserosa

* $P < 0.05$

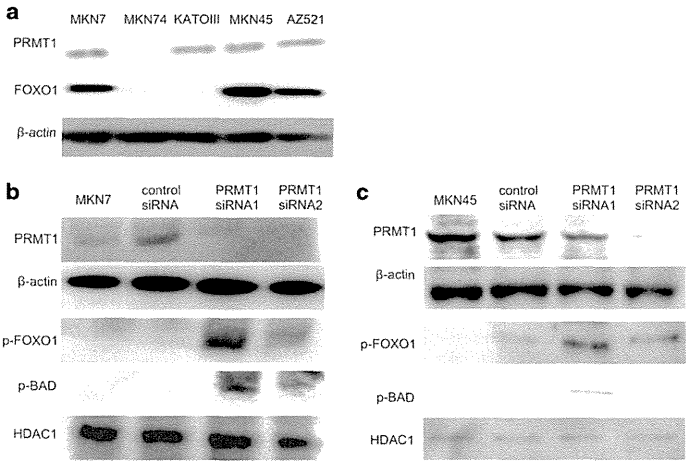

Fig. 3 RNA interference of protein arginine methyltransferase 1 (*PRMT1*) in the gastric cancer cell lines. **a** PRMT1 protein expression was detected in MKN7, KATO-III, MKN45, and AZ521 cells by Western blot analysis. Forkhead box O1 (*FOXO1*) protein expression was detected in MKN7, MKN45, and AZ521 cells by Western blot analysis. β-Actin was used as the loading control. **b**, **c** Western blot analysis of PRMT1, phosphorylated FOXO1 (*p-FOXO1*), and phosphorylated BCL-2 antagonist of cell death (*p-BAD*) in PRMT1small interfering RNA (*siRNA*) cells, control siRNA cells, and parent MKN7 and MKN45 cells. p-FOXO1 and p-BAD proteins were extracted as nuclear proteins. These expression levels of these proteins were normalized to the expression levels of β-actin and nuclear histone deacetylase 1 (*HDAC1*)

The results of our in vitro study show that p-FOXO1 and p-BAD, which are phosphorylated by Akt, were induced in PRMT1 siRNA cells. These phosphorylated proteins are known to be in the inactive forms and transferred to extranuclear cellular compartments. Therefore, we speculated that PRMT1, at least in GC, might function as a tumor suppressor via activation of the tumor suppressors FOXO1 and BAD.

FOXO1 is known to be an important tumor suppressor in several types of cancer cells [4], and we validated the correlation of PRMT1 protein expression and FOXO1 nuclear translocation in clinical GC samples. We focused on FOXO1 as one of the PRMT1 substrates; however, it was reported that methylation by PRMT1 regulates various important cellular functions, not only via suppression of Akt/FOXO1 signaling, but also via other factors, including BAD [11], BRCA1 [24], histones [25], and bone morphogenetic protein [26]. In this study, we showed that PRMT1 suppression induced chemoresistance and nuclear accumulation of p-FOXO1 and p-BAD in GC cell lines, and GC patients with low PRMT1 expression had a significantly higher incidence of recurrence after adjuvant chemotherapy than those with high PRMT1 expression. Similarly to what we observed, PRMT1 has been suggested to be related to drug resistance in acute lymphoblastic leukemia [27] and apoptosis induction [10, 11, 28]. However, PRMT1 was reported to be overexpressed in several cancers; therefore, some researchers have focused on PRMT1 as a potential therapeutic candidate involving a strategy to target PRMT1 by developing specific inhibitors [29–31]. Our results suggest that PRMT1 induction is a promising therapeutic tool; however, further studies are required to determine if PRMT1 should be targeted or induced to overcome refractory cancers.

In conclusion, low PRMT1 expression is associated with a shorter duration of cancer-specific survival and recurrence after adjuvant chemotherapy in patients with GC. PRMT1 expression in patients with GC may be a useful predictor of poor prognosis and recurrence. Moreover, PRMT1 expression is associated with nuclear accumulation of tumor suppressing FOXO1 in clinical GC samples, and chemoresistance is induced by PRMT1 suppression through the inactivation of FOXO1 and BAD. Our results

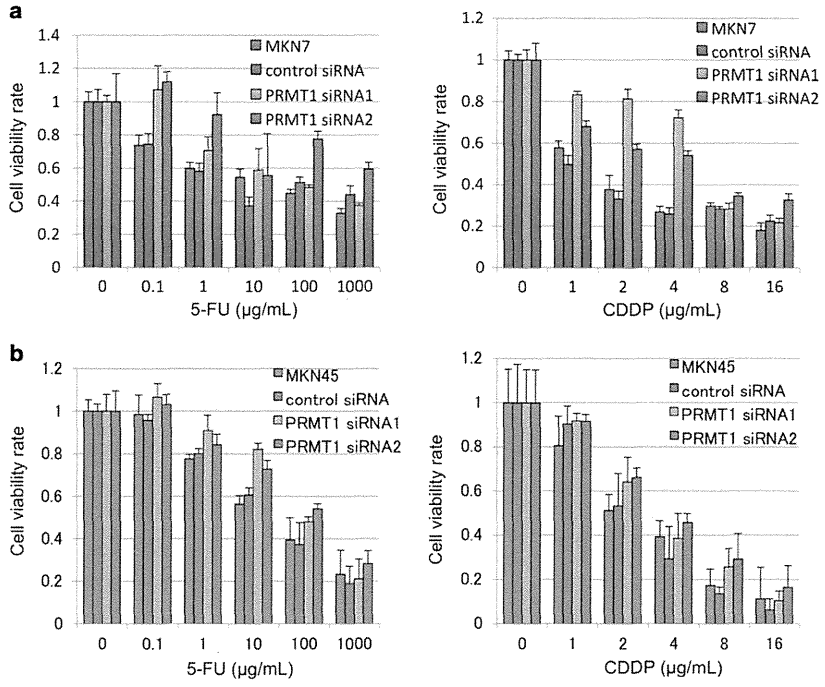

Fig. 4 Cisplatin sensitivity assay with RNA interference of protein arginine methyltransferase 1 (*PRMT1*) in the gastric cancer cell lines. The WST assay was used to evaluate sensitivities to 5- fluorouracil (*5-FU*) and cisplatin (*CDDP*) of MKN7 and MKN45 cells treated with small interfering RNA (*siRNA*) targeting PRMT1 messenger RNA. Cell viability of PRMT1 siRNA (siRNA1, siRNA2) cells was enhanced in comparison with that of control siRNA and parent cells. The data are presented as the mean ± standard deviation

suggest that PRMT1 is a promising therapeutic tool for overcoming refractory GC.

Acknowledgments We thank Yukie Saito, Tomoko Yano, Yuka Matsui, Ayaka Ishida, and Ayaka Ishikubo for their excellent assistance. Masahiko Nishiyama received a research grant from Yakult Honsha and Grants-in-Aid for Scientific Research from the Japan Society for the Promotion of Science: grant numbers 22591450, 23591857, and 15K10085. The work was supported in part by Uehara Zaidan, the Promotion Plan for the Platform of Human Resource Development for Cancer and New Paradigms—Establishing Centers for Fostering Medical Researchers of the Future programs of the Ministry of Education, Culture, Sports, Science and Technology of Japan, and by Gunma University Initiative for Advanced Research.

References

1. Kelley JR, Duggan JM. Gastric cancer epidemiology and risk factors. J Clin Epidemiol. 2003;56:1–9.
2. Sun P, Xiang JB, Chen ZY. Meta-analysis of adjuvant chemotherapy after radical surgery for advanced gastric cancer. Br J Surg. 2009;96:26–33.
3. Sasako M, Sano T, Yamamoto S, et al. D2 lymphadenectomy alone or with para-aortic nodal dissection for gastric cancer. N Engl J Med. 2008;359:453–62.
4. Carter ME, Brunet A. FOXO transcription factors. Curr Biol. 2007;17:R113–4.
5. Han CY, Cho KB, Choi HS, et al. Role of FoxO1 activation in MDR1 expression in adriamycin-resistant breast cancer cells. Carcinogenesis. 2008;29:1837–44.
6. Oh WK, Cho KB, Hien TT, et al. Amurensin G, a potent natural SIRT1 inhibitor, rescues doxorubicin responsiveness via down-regulation of multidrug resistance 1. Mol Pharmacol. 2010;78:855–64.
7. Park J, Ko YS, Yoon J, et al. The forkhead transcription factor FOXO1 mediates cisplatin resistance in gastric cancer cells by activating phosphoinositide 3-kinase/Akt pathway. Gastric Cancer. 2014;17:423–30.
8. Zhang Y, Gan B, Liu D, et al. FoxO family members in cancer. Cancer Biol Ther. 2011;12:253–9.
9. Bedford MT, Richard S. Arginine methylation an emerging regulator of protein function. Mol Cell. 2005;18:263–72.
10. Yamagata K, Daitoku H, Takahashi Y, et al. Arginine methylation of FOXO transcription factors inhibits their phosphorylation by Akt. Mol Cell. 2008;32:221–31.

11. Sakamaki J, Daitoku H, Ueno K, et al. Arginine methylation of BCL-2 antagonist of cell death (BAD) counteracts its phosphorylation and inactivation by Akt. Proc Natl Acad Sci USA. 2011;108:6085–90.
12. Papadokostopoulou A, Mathioudaki K, Scorilas A, et al. Colon cancer and protein arginine methyltransferase 1 gene expression. Anticancer Res. 2009;29:1361–6.
13. Mathioudaki K, Papadokostopoulou A, Scorilas A, et al. The PRMT1 gene expression pattern in colon cancer. Br J Cancer. 2008;99:2094–9.
14. Mathioudaki K, Scorilas A, Ardavanis A, et al. Clinical evaluation of PRMT1 gene expression in breast cancer. Tumour Biol. 2011;32:575–82.
15. Elakoum R, Gauchotte G, Oussalah A, et al. CARM1 and PRMT1 are dysregulated in lung cancer without hierarchical features. Biochimie. 2014;97:210–8.
16. Wang S, Tan X, Yang B, et al. The role of protein arginine-methyltransferase 1 in gliomagenesis. BMB Rep. 2012;45:470–5.
17. Yoshimatsu M, Toyokawa G, Hayami S, et al. Dysregulation of PRMT1 and PRMT6, Type I arginine methyltransferases, is involved in various types of human cancers. Int J Cancer. 2011;128:562–73.
18. Yu Z, Chen T, Hebert J, et al. A mouse PRMT1 null allele defines an essential role for arginine methylation in genome maintenance and cell proliferation. Mol Cell Biol. 2009;29:2982–96.
19. Mitchell TR, Glenfield K, Jeyanthan K, et al. Arginine methylation regulates telomere length and stability. Mol Cell Biol. 2009;29:4918–34.
20. Dhar S, Vemulapalli V, Patananan AN, et al. Loss of the major type I arginine methyltransferase PRMT1 causes substrate scavenging by other PRMTs. Sci Rep. 2013;3:1311.
21. Herrmann F, Fackelmayer FO. Nucleo-cytoplasmic shuttling of protein arginine methyltransferase 1 (PRMT1) requires enzymatic activity. Genes Cells. 2009;14:309–17.
22. Goulet I, Gauvin G, Boisvenue S, et al. Alternative splicing yields protein arginine methyltransferase 1 isoforms with distinct activity, substrate specificity, and subcellular localization. J Biol Chem. 2007;282:33009–21.
23. Rust HL, Subramanian V, West GM, et al. Using unnatural amino acid mutagenesis to probe the regulation of PRMT1. ACS Chem Biol. 2014;9:649–55.
24. Guendel I, Carpio L, Pedati C, et al. Methylation of the tumor suppressor protein, BRCA1, influences its transcriptional cofactor function. PLoS One. 2010;5:e11379.
25. Balint BL, Gabor P, Nagy L. Genome-wide localization of histone 4 arginine 3 methylation in a differentiation primed myeloid leukemia cell line. Immunobiology. 2005;210:141–52.
26. Xu J, Wang AH, Oses-Prieto J, et al. Arginine methylation initiates BMP-induced Smad signaling. Mol Cell. 2013;51:5–19.
27. van Galen JC, Kuiper RP, van Emst L, et al. BTG1 regulates glucocorticoid receptor auto induction in acute lymphoblastic leukemia. Blood. 2010;115:4810–9.
28. Zheng S, Moehlenbrink J, Lu YC, et al. Arginine methylation-dependent reader-writer interplay governs growth control by E2F-1. Mol Cell. 2013;52:37–51.
29. Xie Y, Zhou R, Lian F, et al. Virtual screening and biological evaluation of novel small molecular inhibitors against protein arginine methyltransferase 1 (PRMT1). Org Biomol Chem. 2014;12:9665–73.
30. Yan L, Yan C, Qian K, et al. Diamidine compounds for selective inhibition of protein arginine methyltransferase 1. J Med Chem. 2014;57:2611–22.
31. Hong W, Li J, Laughton CA, et al. Investigating the binding preferences of small molecule inhibitors of human protein arginine methyltransferase 1 using molecular modelling. J Mol Graph Model. 2014;51:193–202.

Ann Surg Oncol (2015) 22:S1566–S1573
DOI 10.1245/s10434-015-4831-6

Annals of
SURGICAL ONCOLOGY
OFFICIAL JOURNAL OF THE SOCIETY OF SURGICAL ONCOLOGY

ORIGINAL ARTICLE – TRANSLATIONAL RESEARCH AND BIOMARKERS

Nuclear PROX1 is Associated with Hypoxia-Inducible Factor 1α Expression and Cancer Progression in Esophageal Squamous Cell Carcinoma

Takehiko Yokobori, MD, PhD[1], Pinjie Bao, MSc[2], Minoru Fukuchi, MD, PhD[2], Bolag Altan, MD, PhD[2], Daigo Ozawa, MD, PhD[2], Susumu Rokudai, PhD[1], Tuya Bai, MSc[2], Yuji Kumakura, MD[2], Hiroaki Honjo, MD[2], Keigo Hara, MD[2], Makoto Sakai, MD, PhD[2], Makoto Sohda, MD, PhD[2], Tatsuya Miyazaki, MD, PhD[2], Munenori Ide, MD, PhD[3], Masahiko Nishiyama, MD, PhD[1], Tetsunari Oyama, MD, PhD[3], and Hiroyuki Kuwano, MD, PhD, FACS[2]

[1]Department of Molecular Pharmacology and Oncology, Gunma University Graduate School of Medicine, Maebashi, Japan; [2]Department of General Surgical Science, Graduate School of Medicine, Gunma University, Maebashi, Japan; [3]Department of Diagnostic Pathology, Graduate School of Medicine, Gunma University, Maebashi, Japan

ABSTRACT

Background. Transcription factor prospero homeobox 1 (PROX1) has been identified as a master regulator of lymphangiogenesis associated with metastasis. Although PROX1 expression has been investigated in several cancers, its clinical significance remains controversial and needs further validation. In this study, we investigated the clinical and functional significance of PROX1 and PROX1 regulator hypoxia-inducible factor 1α (HIF1α) in esophageal squamous cell carcinoma (ESCC).

Methods. A total of 117 samples from ESCC patients were analyzed for PROX1, HIF1α, and E-cadherin expression by immunohistochemistry; correlation with clinicopathological characteristics was determined. PROX1 function was evaluated in PROX1 small interfering RNA (siRNA)-transfected human ESCC cells in vitro by assessing cell proliferation and migration.

Results. PROX1 expression was higher in ESCC than in normal tissues. Patients with higher PROX1 expression ($n = 26$) had increased nuclear accumulation of HIF1α ($p = 0.004$) and more advanced metastasis, both lymph node (N factor; $p = 0.09$) and hematogenous (M factor; $p = 0.04$), than those with lower PROX1 expression ($n = 91$). In addition, high PROX1 and HIF1α expression correlated with low levels of E-cadherin, an epithelial cell marker. Analysis of overall and cancer-specific survival indicated that elevated PROX1 expression was significantly correlated with poor prognosis ($p = 0.0064$). PROX1 downregulation in ESCC cells inhibited cellular proliferation and migration ($p < 0.05$). Hypoxia restored PROX1 levels that were reduced by *PROX1*-specific siRNA.

Conclusion. Our data suggest that high expression of PROX1 in ESCC could be used as an indicator of poor prognosis, and that PROX1 is a promising candidate molecular target for ESCC treatment.

Takehiko Yokobori and Pinjie Bao contributed equally to this work.

Electronic supplementary material The online version of this article (doi:10.1245/s10434-015-4831-6) contains supplementary material, which is available to authorized users.

First Received: 19 March 2015;
Published Online: 27 August 2015

T. Yokobori, MD, PhD
e-mail: bori45@gunma-u.ac.jp

M. Fukuchi, MD, PhD
e-mail: mfukuchi@saitama-med.ac.jp

Esophageal squamous cell carcinoma (ESCC) is a cancer with poor prognosis because of early lymph node metastasis and hematogenous metastasis.[1–3] Therefore, patients with ESCC tend to relapse more frequently compared with those with other gastrointestinal cancers, even after radical resection. To provide optimal treatments and postoperative surveillance for high-risk ESCC patients, a reliable diagnostic and prognostic biomarker for the prediction of cancer recurrence in these patients is required. Moreover, such a marker might be a promising molecular target to control ESCC progression.

Lymphangiogenesis is very important for the establishment of lymph node metastases.[4] Therefore, lymphatic endothelial cell markers such as prospero homeobox 1 (PROX1), vascular endothelial growth factor receptor 3 (VEGFR3), and forkhead box protein C2 (FOXC2) appear to be essential for lymphatic vessel growth and have been investigated in relation to metastatic potential in several cancers.[5,6] In particular, PROX1 has been identified as a master regulator of lymphangiogenesis via induction of VEGFR3 and FOXC2 expression.[7,8] The clinical significance of PROX1 in human solid cancers is controversial, and PROX1 expression has been associated with cancer progression and poor prognosis in hepatocellular carcinoma,[9] colon cancer,[10,11] and malignant astrocytic gliomas.[12] In addition, PROX1 has been reported as a tumor suppressor candidate in hepatocellular carcinoma,[13] neuroblastoma,[14] breast cancer,[15] and pancreatic cancer,[16] suggesting that the oncogenic potential of PROX1 is cancer type-dependent.

In ESCC, the clinical significance of PROX1 is even less clear. A study on human esophageal cancer cells found a loss-of-function RNA mutation in PROX1;[17] it has also been shown that PROX1 suppresses interferon-γ-induced antiproliferative activity in these cells.[18] Thus, the role of PROX1 in ESCC has not been established.

A previous study has demonstrated that PROX1 functions as a stimulator of expression and protein stability of hypoxia-inducible factor 1α (HIF1α).[9] In turn, HIF1α and HIF2α have been reported to activate PROX1 expression.[19] HIF1α, a transcription factor playing an essential role in cellular responses to hypoxia, has been found to regulate epithelial-mesenchymal transition (EMT) and cancer stem cell properties, and to be associated with the recurrence and poor prognosis in several cancers.[20] Therefore, HIF1α has been viewed as a potential target in the treatment of refractory cancers. However, the relationship between HIF1α and PROX1 expression and clinicopathological parameters in ESCC has not yet been investigated.

The purpose of this research was to study the function and clinical significance of PROX1 in ESCC. We examined PROX1 and HIF1α expression in ESCC tissues using immunohistochemistry to evaluate prognostic potential of PROX1 expression in ESCC. Moreover, we inhibited PROX1 expression in ESCC cells in vitro to determine whether PROX1 can be a treatment target in ESCC.

MATERIALS AND METHODS

Clinical Samples and Cell Lines

Surgical specimens were obtained from 117 ESCC patients (103 males and 14 females) who had undergone potentially curative surgery at the Department of General Surgical Science, Gunma University, between 1991 and 2009. Informed consent was obtained according to the Ethical Guidelines for Medical and Health Research Involving Human Subjects (Ministry of Health, Labor and Welfare, and Ministry of Education, Culture, Sports, Science and Technology [MEXT], Japan, 2015). Protocol approval was obtained from an independent review board at Gunma University Hospital. The mean patient age was 63.1 years (range 42–80 years), and the median follow-up period for survivors was 30.3 months (range 1–113 months). ESCC pathological stage was determined based on the 6th edition of the TNM classification of the Union for International Cancer Control (UICC). None of the patients had received irradiation or chemotherapy prior to surgery, or had hematogenous metastases at the time of surgery.

Human ESCC cell lines KYSE140,[21] TE1, TE8, and TE15 were provided by the Japanese Collection of Research Bioresources (JCRB) cell bank and RIKEN BRC through the National Bio-Resource Project of MEXT, Japan. TE8 cells were cultured in RPMI-1640 supplemented with penicillin/streptomycin, and 10 % fetal bovine serum (FBS) in a humidified 5 % CO_2 incubator at 37 °C. Cells were subjected to hypoxia (1 % O_2) using the BIONIX-1 hypoxic culture kit (Sugiyama-Gen, Tokyo, Japan), and were not cross-contaminated with other cell lines as confirmed by short tandem repeat polymerase chain reaction (STR-PCR) in the JCRB cell bank and RIKEN BioResource Center.

Immunohistochemistry

An ESCC tissue microarray was prepared using surgically resected specimens, including noncancerous tissues. Immunohistochemistry was performed as previously described.[22] Two sequential 2-μm slides of each sample were treated with primary antibodies against PROX1 (1:100) and HIF1α (1:300) (both from Abcam, Tokyo, Japan), for 24 h at 4 °C. Negative control slides were incubated without the primary antibodies, and no detectable staining was observed.

Nuclear levels of PROX1 and HIF1α were evaluated as follows: low expression (0, no staining; 1, weak staining) and high expression (2, moderate-to-strong nuclear staining) (Electronic Supplementary Fig. 1).

Fluorescent Immunohistochemistry

After endogenous peroxidase was blocked, the sections were boiled in citrate buffer (pH 6.4) for 15 min in a microwave. Nonspecific binding sites were blocked by incubation with Protein Block Serum-Free Reagent for 30 min, and the sections were incubated with the primary antibodies against PROX1 (1:400), HIF1α (1:1000), and E-cadherin (1:500; Cell Signaling Technology, Tokyo,

Japan) for 1 h at room temperature. Multiplex covalent labeling (PROX1, cyanine 3; HIF1α and E-cadherin, fluorescein) with tyramide signal amplification (Opal™ 3-Plex Kit; Perkin Elmer, Waltham, MA, USA) was performed according to the manufacturer's protocol. All sections were counterstained with DAPI and examined under an All-in-One BZ-X710 fluorescence microscope (Keyence Corporation, Osaka, Japan).

PROX1 RNA Interference

PROX1-specific small interfering RNA (siRNA) [Silencer Pre-Designed siRNA] purchased from Bonac Corporation (Kurume, Fukuoka, Japan) was mixed with HilyMax transfection reagent (Dojindo Laboratories, Kumamoto, Japan) in six-well flat-bottom microtiter plates. TE8 cells were seeded in 2 mL RPMI-1640 in the microtiter plates and incubated with siRNAs at 37 °C for 24 h before analysis using Western blot.

Protein Extraction and Western Blotting

Total proteins were extracted from ESCC cells using PRO-PREP (iNtRON Biotechnology, Kyungki-Do, Korea), separated by SDS-PAGE using 10 % gels, and transferred to membranes which were incubated overnight at 4 °C with the antibodies against PROX1 (1:2000), HIF1α (1:1000), and β-actin (1:4000) [Sigma, St. Louis, MO, USA], followed by horseradish peroxidase-conjugated secondary antibodies. Specific signals were detected using the ECL Prime Western Blotting Detection System (GE Healthcare, Tokyo, Japan) and quantified using an Image Quant LAS 4000 instrument (GE Healthcare).

In Vitro Proliferation Assay

TE8 cells transfected for 48 h were plated in 96-well plates (3.0×10^4 cells/well) in 10 % FBS–RPMI-1640. After 48 h, 10 μL of CCK-8 solution (CCK-8; Dojindo Laboratories) was added to each well for 2 h at 37 °C, and the absorbance was detected at 450 nm using an xMark™ Microplate Absorbance Spectrophotometer (Bio Rad, Hercules, CA, USA).

In Vitro Migration Assay

Cell migration was analyzed by chemotaxis assay using 24-well Falcon Cell Culture Inserts (pore size, 8 μm). TE8 cells (8.0×10^4) were seeded in the upper chamber, and the lower chamber was filled with 750 μL of 10 % FBS–RPMI-1640. After 24 h incubation at 37 °C, the cells that migrated to the lower surface of the filter were fixed with 4 % paraformaldehyde, stained with Giemsa Stain Solution (Wako, Osaka, Japan), and then counted under a microscope. A total of six randomly chosen fields were evaluated in duplicate assays.

Statistical Analysis

For continuous variables, the data were expressed as mean ± SD. The association between PROX1 and HIF1α expression and clinicopathological factors, as well as the in vitro data, was analyzed using Student's *t* test, Chi square test, and analysis of variance (ANOVA). Overall and cancer-specific survival were measured from the day of surgery and plotted according to the Kaplan–Meier method; the log-rank test was used for comparison. Differences were considered statistically significant at $p < 0.05$. Cox proportional hazards regression was used to test PROX1 independent prognostic contribution. All statistical analyses were performed using the JMP software package (SAS Institute Inc., Cary, NC, USA).

RESULTS

Immunohistochemical Analysis of (Prospero Homeobox 1 (PROX1) and Hypoxia-Inducible Factor 1α (HIF1α) Expression in Esophageal Squamous Cell Carcinoma (ESCC) Tissues

PROX1 and HIF1α nuclear expression in ESCC specimens was evaluated by immunohistochemistry. PROX1 expression was scored high in 26 (22.2 %) ESCC samples and low in 91 (77.8 %) ESCC samples, while HIF1α expression was scored high in 42 (35.9 %) ESCC samples and low in 75 (64.1 %) ESCC samples; representative images are shown in Fig. 1. Our analysis revealed a direct correlation between HIF1α and PROX1 nuclear expression, i.e. patients with high PROX1 demonstrated higher HIF1α levels than those with low PROX1 expression (Fig. 1).

In normal esophageal epithelium, PROX1 and HIF1α immunofluorescence was almost undetected (Fig. 1b), but in ESCC tissues, both transcription factors were significantly upregulated (Fig. 1c). Expression of the epithelial marker E-cadherin was examined to validate the relationship between EMT, PROX1, and HIF1α in ESCC. The results indicate that in almost all ESCC cells, E-cadherin expression was not co-localized with that of PROX1 and HIF1α (Electronic Supplementary Fig. 2a, b, respectively).

Association Between PROX1 Expression and Clinicopathological Features of ESCC

Correlations between PROX1 expression, patients' clinicopathological characteristics (age, sex, tumor location

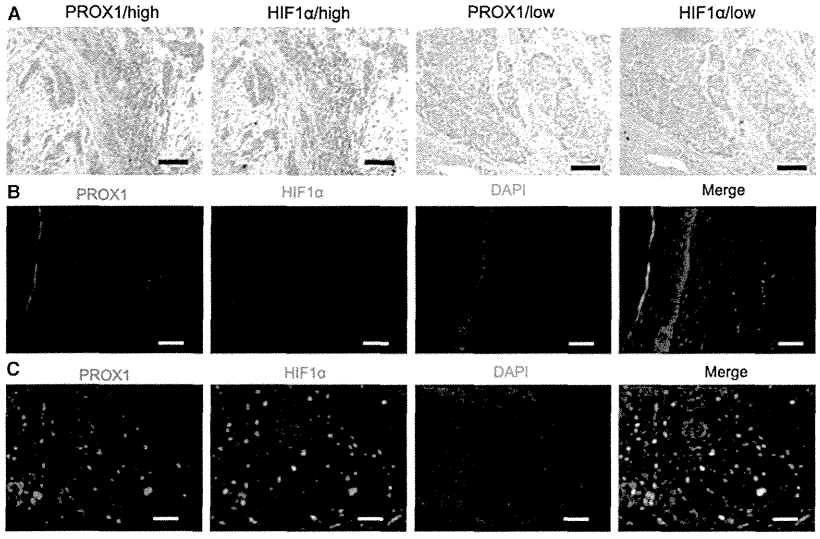

FIG. 1 Immunostaining analysis of PROX1 and HIF1α expression in ESCC tissue samples. **a** Deparaffinized sections of ESCC tumors were stained with anti-PROX1 and anti-HIF1α antibodies and counterstained with hematoxylin. *Left panels*: ESCC patients with high levels of PROX1 expression in tumors demonstrated enhanced HIF1α expression. *Right panels* ESCC patients with low levels of PROX1 expression in tumors demonstrated decreased HIF1α expression. Original magnification: ×100; scale bar, 100 μm. **b**, **c** Noncancerous squamous epithelial cells (**b**) and ESCC cells (**c**) were immunostained with the antibodies against PROX1 (*red*) and HIF1α (*green*). All sections were counterstained with DAPI (*blue*). *Scale bar* 50 μm. *PROX1* prospero homeobox 1, *HIF1α* hypoxia-inducible factor 1α, *ESCC* esophageal squamous cell carcinoma

and histology, T, N and M factors, lymphatic and venous invasion, and pathological stage), and HIF1α levels are shown in Table 1. The results indicate that patients with high and low PROX1 expression in tumors differed in HIF1α levels and metastasis: the first group had increased HIF1α nuclear accumulation ($p = 0.004$) and a higher degree of metastasis, both in regional lymph nodes (N factor; $p = 0.09$) and distant tissues (M factor; $p = 0.04$). However, no significant differences were observed in age, sex, tumor location and histology, T factor, lymphatic and venous invasion, or pathological stage.

Prognostic Significance of PROX1 Expression in ESCC Patients

Overall survival and cancer-specific survival of ESCC patients with high PROX1 tumors was significantly lower than that of patients with low PROX1 tumors ($p = 0.01$ and $p = 0.005$, respectively) (Fig. 2a, b). Multivariate analysis indicated that high PROX1 expression in ESCC tissues was an independent prognostic marker of poor survival, similar to T and N factors ($p = 0.0064$) (Electronic Supplementary Table 1).

The results were consistent with overall and cancer-specific survival of ESCC patients with high HIF1α expression in tumors, which were significantly lower than that of patients with low HIF1α expression ($p = 0.0022$ and $p = 0.0155$, respectively) (Electronic Supplementary Fig. 3a, b).

PROX1-Specific Small Interfering RNA (siRNA) Inhibits Cancer Cell Proliferation and Migration In Vitro

PROX1 was found to be highly expressed in all analyzed ESCC cell lines (Fig. 3a). We chose two *PROX1*-specific siRNAs (siRNA1 and siRNA2) to investigate the effect of PROX1 inhibition on functional parameters in TE8 cells. Both species of *PROX1* siRNA significantly reduced PROX1 levels compared with control siRNAs; however, the effect was abrogated when TE8 cells were subjected to hypoxia, which restored PROX1 expression to control levels (Fig. 3b and Electronic Supplementary Fig. 4a). In normoxic conditions, HIF1α protein was not detected in *PROX1* siRNA-transfected TE8 cells (data not shown); however, it was elevated in hypoxic cells (Fig. 3b and Electronic Supplementary Fig. 4b). The reduction in

TABLE 1 Clinicopathological characteristics and HIF1α nuclear levels in 117 ESCC patients stratified by PROX1 expression

Factors	Nulclear PROX1 expression		*p* value
	Low $n = 91$	High $n = 26$	
Age	62.5 ± 8.1	65.2 ± 6.8	0.12
Gender			
Male	80	23	1
Female	11	3	
Location			
Cervical	0	1	0.4
Upper thoracic	11	4	
Middle thoracic	38	10	
Lower thoracic	37	9	
Abdominal	5	2	
Histology			
Well	21	2	0.16
Moderate	50	19	
Poorly	20	5	
T factor			
T1	19	4	0.36
T2	10	6	
T3	58	14	
T4	4	2	
N factor			
Absent	22	2	0.09**
Present	69	24	
M factor			
M0	61	17	0.04*
M1a	9	0	
M1b	15	9	
Lymphatic invasion			
Absent	2	1	0.53
Present	88	25	
Venous invasion			
Absent	11	5	0.34
Present	79	21	
Stage			
I, II	35	7	0.35
III, IV	56	19	
HIF-1α nuclear expression			
Low	65	10	0.004*
High	26	16	

* $p < 0.05$; ** $p < 0.1$

PROX1 expression significantly inhibited ESCC cell proliferation (Fig. 3c) and migration (Fig. 3d), indicating the involvement of PROX1 in the ability of cancer cells to metastasize.

DISCUSSION

In this study, we demonstrated that high PROX1 expression correlated with the increase in HIF1 and decrease in E-cadherin levels, and also with cancer progression, and that PROX1 expression is an independent prognostic factor for ESCC patients. These results are supported by the findings in vitro showing that PROX1 regulates proliferation and migration of ESCC cells.

PROX1 expression in ESCC tumors was higher than that in noncancerous tissues. PROX1 is known to be regulated by the hypoxia-induced transcription factors HIF1α and HIF2α,[19] COUP-TFII,[23] NF-κB,[24] SOX18,[25] and HOXD8,[7] as well as by Kaposi sarcoma herpes virus[26] in vascular endothelial cells and cancer cells. In ESCC tumors, the expression of HIFs[27] and NF-κB[28] was higher than in noncancerous tissues, and was associated with cancer progression, therapeutic resistance, and poor outcome. In this study, we showed that hypoxia induced PROX1 expression in *PROX1* siRNA-transfected cancer cells, suggesting that in ESCC, PROX1 may be one of the important downstream target genes regulated by hypoxia-induced transcription factors and NF-κB in promoting cancer progression.

PROX1 expressed in lymphatic endothelial cells is considered to play an important role in lymphangiogenesis.[29,30] In cancer patients, high PROX1 expression was correlated with lymphatic invasion and lymph node metastasis (N factor).[31,32] In our study, no significant association of high PROX1 expression with lymphatic invasion was found; however, it tended to correlate with N factor. The reason might be that, among the 117 ESCC patients, only three did not have lymphatic invasion. To investigate the relationship between PROX1 and lymphatic invasion in ESCC, it may be important to evaluate PROX1 expression in early ESCC.

Cancer development depends on the metastatic cascade characterized by the induction of EMT in migrating cancer cells originating from both primary tumors and metastatic sites.[33–35] EMT is induced by many cancer-related signaling molecules, including HIF1, NF-κB, FOXC2, TGF-β, integrins, Wnt/β-catenin, receptor tyrosine kinases, Notch, matrix metalloproteinases, and microRNAs.[33,36] Previous reports indicate that PROX1 regulates some of these EMT inducers, including HIF1,[37] FOXC2,[7] integrin α9,[38,39] β-catenin/TCF,[10] and microRNA-9.[11] In this study, ESCC patients with high PROX1 expression also demonstrated increased HIF1α nuclear accumulation, reduced expression of epithelial marker E-cadherin, and increased lymph node and hematogenous metastases, while cancer cells with inhibited PROX1 expression demonstrated slower proliferation and migration. These findings indicate that in

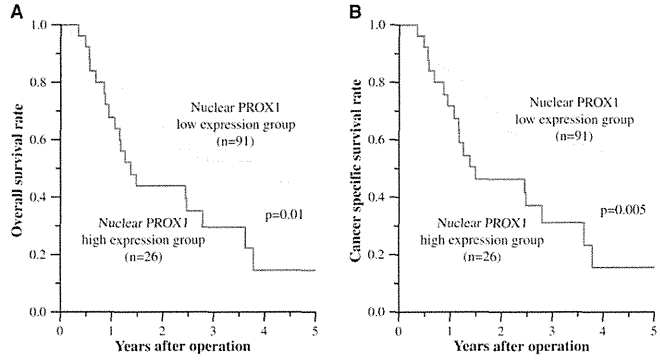

FIG. 2 Correlation of postoperative survival with PROX1 expression. **a** Overall survival of ESCC patients according to PROX1 expression in the nuclei. ESCC patients with high PROX1 expression in tumors ($n = 26$) had significantly lower overall survival compared with those with low PROX1 expression ($n = 91$; $p = 0.01$). **b** Cancer-specific survival of ESCC patients according to PROX1 expression in the nuclei. ESCC patients with high PROX1 expression had significantly lower cancer-specific survival compared with those with low PROX1 expression ($p = 0.005$). *PROX1* prospero homeobox 1, *ESCC* esophageal squamous cell carcinoma

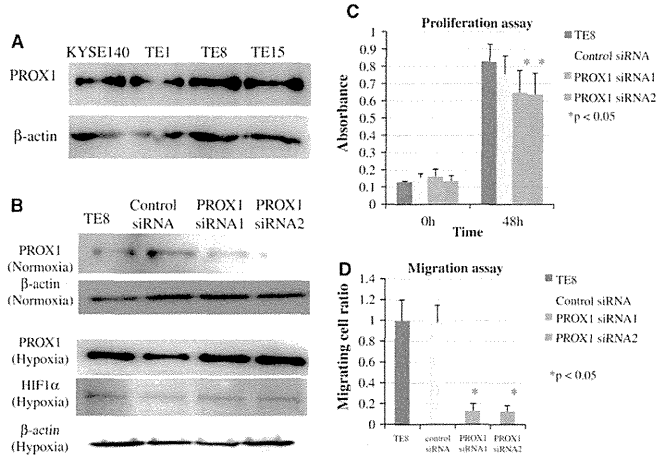

FIG. 3 Proliferation and migration of ESCC cells transfected with *PROX1*-specific siRNA. **a** PROX1 expression in the ESCC cell lines KYSE140, TE1, TE8, and TE15 was analyzed using Western blotting; β-actin was used as a loading control. **b** TE8 cells were transfected with *PROX1*-specific siRNA (PROX1 siRNA1 and 2), and protein expression was analyzed using Western blotting; β-actin was used as a loading control. In normal conditions (normoxia, *upper panels*), PROX1 expression was reduced in *PROX1* siRNA-transfected TE8 cells. In the cells subjected to hypoxic conditions, the expression of PROX1 and HIF1α was induced (*lower panels*). **c** Proliferation of TE8 cells was analyzed using the CCK-8 assay. **d** Migration of TE8 cells was analyzed using the chemotaxis assay. TE8 cells transfected with *PROX1*-specific siRNA showed significantly reduced proliferation and migration compared with control siRNA-transfected and wild-type TE8 cells. Data are expressed as mean ± SD. *ESCC* esophageal squamous cell carcinoma, *PROX1* prospero homeobox 1, *siRNA* small-interfering RNA, *CCK-8* Cell Counting Kit-8, *HIF1α* hypoxia-inducible factor 1α, * indicates $p < 0.05$

ESCC, PROX1 regulates metastatic potential by inducing EMT via HIF1α.

Importantly, our data also suggest that PROX1 may be a promising prognostic biomarker and a new candidate for targeted therapy in ESCC. PROX1 has been shown to have dual functions as a tumor suppressor and tumor promoter in several cancers.[9,16–18] In search of the explanation for functionally diverse roles of PROX1 in cancer, we noted a report that PROX1 inhibited proliferation of hepatocellular carcinoma cells by inducing p53-dependent senescence-like phenotype, suggesting a relationship of PROX1 with cell proliferation.[40] Using next-generation sequencing analysis, other studies have reported that the frequency of p53 mutations in ESCC (92 %) is much higher than that in hepatocellular carcinoma (20.8 %).[41,42] PROX1 functions as a tumor suppressor in hepatocellular carcinoma and neuroblastoma, where p53 somatic mutations are rare.[43] These findings suggest that p53 status may regulate PROX1 function in cancer cells. In this study, PROX1 knockdown in TE8 cells harboring p53 mutations inhibited cell proliferation and migration. Although PROX1 has been demonstrated to act as a tumor suppressor, our results strongly suggest that PROX1 expression is associated with poor prognosis and can be a new therapeutic target in patients with p53-mutated ESCC tumors.

CONCLUSIONS

Elevated PROX1 expression is a factor contributing to shorter survival in ESCC patients, and may be used as a prediction biomarker for poor prognosis. PROX1 expression was associated with both local lymph node and distant metastases in ESCC patients, and with the ability for proliferation and migration of ESCC cells. Our results suggest that PROX1 may be a promising molecular target in ESCC.

ACKNOWLEDGMENT This work was supported by the Promotion Plan for the platform of Human Resource Development for Cancer and New Paradigms–Establishing Centers for Fostering Medical Researchers of the Future; programs of the Ministry of Education, Culture, Sports, Science and Technology of Japan; Gunma University Initiative for Advanced Research (GIAR); and Grants-in-Aid for Scientific Research from the Japan Society for the Promotion of Science (JSPS; Grant Numbers 21591690, 22591450, 23591857, 15K10085, and 15K20902).

DISCLOSURE Masahiko Nishiyama has received a research Grant from Yakult Honsha Co. Ltd.

REFERENCES

1. Napier KJ, Scheerer M, Misra S. Esophageal cancer: a review of epidemiology, pathogenesis, staging workup and treatment modalities. *World J Gastrointest Oncol.* 2014;6(5):112–20.
2. Kato H, Fukuchi M, Miyazaki T, et al. Surgical treatment for esophageal cancer. Current issues. *Dig Surg.* 2007;24(2):88–95.
3. Enzinger PC, Mayer RJ. Esophageal cancer. *N Engl J Med.* 2003;349(23):2241–52.
4. Karatzanis AD, Koudounarakis E, Papadakis I, Velegrakis G. Molecular pathways of lymphangiogenesis and lymph node metastasis in head and neck cancer. *Eur Arch Otorhinolaryngol.* 2012;269(3):731–7.
5. Nishida N, Mimori K, Yokobori T, et al. FOXC2 is a novel prognostic factor in human esophageal squamous cell carcinoma. *Ann Surg Oncol.* 2011;18(2):535–42.
6. He Y, Karpanen T, Alitalo K. Role of lymphangiogenic factors in tumor metastasis. *Biochim Biophys Acta.* 2004;1654(1):3–12.
7. Harada K, Yamazaki T, Iwata C, et al. Identification of targets of Prox1 during in vitro vascular differentiation from embryonic stem cells: functional roles of HoxD8 in lymphangiogenesis. *J Cell Sci.* 2009;122(Pt 21):3923–30.
8. Hong YK, Harvey N, Noh YH, et al. Prox1 is a master control gene in the program specifying lymphatic endothelial cell fate. *Dev Dyn.* 2002;225(3):351–7.
9. Liu Y, Zhang JB, Qin Y, et al. PROX1 promotes hepatocellular carcinoma metastasis by way of up-regulating hypoxia-inducible factor 1alpha expression and protein stability. *Hepatology.* 2013;58(2):692–705.
10. Petrova TV, Nykanen A, Norrmen C, et al. Transcription factor PROX1 induces colon cancer progression by promoting the transition from benign to highly dysplastic phenotype. *Cancer Cell.* 2008;13(5):407–19.
11. Lu MH, Huang CC, Pan MR, Chen HH, Hung WC. Prospero homeobox 1 promotes epithelial-mesenchymal transition in colon cancer cells by inhibiting E-cadherin via miR-9. *Clin Cancer Res.* 2012;18(23):6416–25.
12. Elsir T, Eriksson A, Orrego A, Lindstrom MS, Nister M. Expression of PROX1 Is a common feature of high-grade malignant astrocytic gliomas. *J Neuropathol Exp Neurol.* 2010; 69(2):129–38.
13. Shimoda M, Takahashi M, Yoshimoto T, Kono T, Ikai I, Kubo H. A homeobox protein, prox1, is involved in the differentiation, proliferation, and prognosis in hepatocellular carcinoma. *Clin Cancer Res.* 2006;12(20 Pt 1):6005–11.
14. Foskolou IP, Stellas D, Rozani I, Lavigne MD, Politis PK. Prox1 suppresses the proliferation of neuroblastoma cells via a dual action in p27-Kip1 and Cdc25A. *Oncogene.* 2013;32(8): 947–60.
15. Versmold B, Felsberg J, Mikeska T, et al. Epigenetic silencing of the candidate tumor suppressor gene PROX1 in sporadic breast cancer. *Int J Cancer.* 2007;121(3):547–54.
16. Schneider M, Buchler P, Giese N, et al. Role of lymphangiogenesis and lymphangiogenic factors during pancreatic cancer progression and lymphatic spread. *Int J Oncol.* 2006;28(4): 883–90.
17. Yoshimoto T, Takahashi M, Nagayama S, et al. RNA mutations of prox1 detected in human esophageal cancer cells by the shifted termination assay. *Biochem Biophys Res Commun.* 2007;359(2): 258–62.
18. Akagami M, Kawada K, Kubo H, et al. Transcriptional factor Prox1 plays an essential role in the antiproliferative action of interferon-gamma in esophageal cancer cells. *Ann Surg Oncol.* 2011;18(13):3868–77.
19. Zhou B, Si W, Su Z, Deng W, Tu X, Wang Q. Transcriptional activation of the Prox1 gene by HIF-1alpha and HIF-2alpha in response to hypoxia. *FEBS Lett.* 2013;587(6):724–31.
20. Keith B, Johnson RS, Simon MC. HIF1alpha and HIF2alpha: sibling rivalry in hypoxic tumour growth and progression. *Nat Rev Cancer.* 2012;12(1):9–22.

21. Shimada Y, Imamura M, Wagata T, Yamaguchi N, Tobe T. Characterization of 21 newly established esophageal cancer cell lines. *Cancer.* 1992;69(2):277–84.
22. Yokobori T, Yokoyama Y, Mogi A, et al. FBXW7 mediates chemotherapeutic sensitivity and prognosis in NSCLCs. *Mol Cancer Res.* 2014;12(1):32–37.
23. Aranguren XL, Beerens M, Coppiello G, et al. COUP-TFII orchestrates venous and lymphatic endothelial identity by homo- or hetero-dimerisation with PROX1. *J Cell Sci.* 2013;126(Pt 5):1164–75.
24. Flister MJ, Wilber A, Hall KL, et al. Inflammation induces lymphangiogenesis through up-regulation of VEGFR-3 mediated by NF-kappaB and Prox1. *Blood.* 2010;115(2):418–29.
25. Francois M, Caprini A, Hosking B, et al. Sox18 induces development of the lymphatic vasculature in mice. *Nature.* 2008; 456(7222):643–7.
26. Yoo J, Lee HN, Choi I, et al. Opposing regulation of PROX1 by interleukin-3 receptor and NOTCH directs differential host cell fate reprogramming by Kaposi sarcoma herpes virus. *PLoS Pathog.* 2012;8(6):e1002770.
27. Kurokawa T, Miyamoto M, Kato K, et al. Overexpression of hypoxia-inducible-factor 1alpha(HIF-1alpha) in oesophageal squamous cell carcinoma correlates with lymph node metastasis and pathologic stage. *Br J Cancer.* 2003;89(6):1042–7.
28. Izzo JG, Malhotra U, Wu TT, et al. Association of activated transcription factor nuclear factor kappab with chemoradiation resistance and poor outcome in esophageal carcinoma. *J Clin Oncol.* 2006;24(5):748–54.
29. Wigle JT, Harvey N, Detmar M, et al. An essential role for Prox1 in the induction of the lymphatic endothelial cell phenotype. *EMBO J.* 2002;21(7):1505–13.
30. Pan MR, Chang TM, Chang HC, Su JL, Wang HW, Hung WC. Sumoylation of Prox1 controls its ability to induce VEGFR3 expression and lymphatic phenotypes in endothelial cells. *J Cell Sci.* 2009;122(Pt 18):3358–64.
31. Lv T, Liu Y, Zhang J, et al. Impact of an altered PROX1 expression on clinicopathology, prognosis and progression in renal cell carcinoma. *PloS One.* 2014;9(5):e95996.
32. Taban O, Cimpean AM, Raica M, Olariu S. PROX1 expression in gastric cancer: from hypothesis to evidence. *Anticancer Res.* 2014;34(7):3439–46.
33. Polyak K, Weinberg RA. Transitions between epithelial and mesenchymal states: acquisition of malignant and stem cell traits. *Nat Rev Cancer.* 2009;9(4):265–73.
34. Bellovin DI, Bates RC, Muzikansky A, Rimm DL, Mercurio AM. Altered localization of p120 catenin during epithelial to mesenchymal transition of colon carcinoma is prognostic for aggressive disease. *Cancer Res.* 2005;65(23):10938–45.
35. Bellovin DI, Simpson KJ, Danilov T, et al. Reciprocal regulation of RhoA and RhoC characterizes the EMT and identifies RhoC as a prognostic marker of colon carcinoma. *Oncogene.* 2006;25(52): 6959–67.
36. Hollier BG, Tinnirello AA, Werden SJ, et al. FOXC2 expression links epithelial-mesenchymal transition and stem cell properties in breast cancer. *Cancer Res.* 2013;73(6):1981–92.
37. Sun S, Ning X, Zhang Y, et al. Hypoxia-inducible factor-1alpha induces Twist expression in tubular epithelial cells subjected to hypoxia, leading to epithelial-to-mesenchymal transition. *Kidney Int.* 2009;75(12):1278–87.
38. Sun X, Fa P, Cui Z, et al. The EDA-containing cellular fibronectin induces epithelial-mesenchymal transition in lung cancer cells through integrin alpha9beta1-mediated activation of PI3-K/AKT and Erk1/2. *Carcinogenesis.* 2014;35(1):184–91.
39. Mishima K, Watabe T, Saito A, et al. Prox1 induces lymphatic endothelial differentiation via integrin alpha9 and other signaling cascades. *Mol Biol Cell.* 2007;18(4):1421–9.
40. Chang TM, Hung WC. The homeobox transcription factor Prox1 inhibits proliferation of hepatocellular carcinoma cells by inducing p53-dependent senescence-like phenotype. *Cancer Biol Ther.* 2013;14(3):222–9.
41. Agrawal N, Jiao Y, Bettegowda C, et al. Comparative genomic analysis of esophageal adenocarcinoma and squamous cell carcinoma. *Cancer Discov.* 2012;2(10):899–905.
42. Guichard C, Amaddeo G, Imbeaud S, et al. Integrated analysis of somatic mutations and focal copy-number changes identifies key genes and pathways in hepatocellular carcinoma. *Nat Genet.* 2012;44(6):694–8.
43. Pugh TJ, Morozova O, Attiyeh EF, et al. The genetic landscape of high-risk neuroblastoma. *Nat Genet.* 2013;45(3):279–84.

PLOS | ONE

RESEARCH ARTICLE

The *A* Allele at rs13419896 of *EPAS1* Is Associated with Enhanced Expression and Poor Prognosis for Non-Small Cell Lung Cancer

Andika C. Putra[1☯], Hidetaka Eguchi[2☯], Kian Leong Lee[3], Yuko Yamane[1], Ewita Gustine[1], Takeshi Isobe[4], Masahiko Nishiyama[5], Keiko Hiyama[6], Lorenz Poellinger[3,7], Keiji Tanimoto[1]*

1 Department of Radiation Medicine, Research Institute for Radiation Biology and Medicine, Hiroshima University, Hiroshima, Japan, **2** Division of Translational Research, Research Center for Genomic Medicine, Saitama Medical University, Saitama, Japan, **3** Cancer Science Institute of Singapore, National University of Singapore, Singapore, Singapore, **4** Division of Clinical Oncology and Respiratory Medicine, Department of Internal Medicine, School of Medicine, Shimane University, Shimane, Japan, **5** Department of Molecular and Cellular Pharmacology, Graduate School of Medicine, Gunma University, Gunma, Japan, **6** Natural Science Center for Basic Research and Development, Hiroshima University, Hiroshima, Japan, **7** Department of Cell and Molecular Biology, Medical Nobel Institute, Karolinska Institute, Stockholm, Sweden

☯ These authors contributed equally to this work.
* ktanimo@hiroshima-u.ac.jp

OPEN ACCESS

Citation: Putra AC, Eguchi H, Lee KL, Yamane Y, Gustine E, Isobe T, et al. (2015) The *A* Allele at rs13419896 of *EPAS1* Is Associated with Enhanced Expression and Poor Prognosis for Non-Small Cell Lung Cancer. PLoS ONE 10(8): e0134496. doi:10.1371/journal.pone.0134496

Editor: Tiffany Seagroves, University of Tennessee Health Science Center, UNITED STATES

Received: April 2, 2015

Accepted: July 9, 2015

Published: August 11, 2015

Data Availability Statement: All relevant data are within the paper and its Supporting Information files.

Funding: This work was partly supported by Grant-in-Aid for Scientific Research (C) (No. 23592766) from Japan Society for the Promotion of Science (JSPS), Grants-in-Aid for Scientific Research on "Innovative Areas (No. 221S0001)" from Japanese Ministry of Education, Culture, Sports, Science and Technology, and the Strategic Research Foundation Grant-aided Project for Private Universities, MEXT. The funders had no role in study design, data

Abstract

Hypoxia-inducible factor-2α (HIF-2α, or EPAS1) is important for cancer progression, and is a putative biomarker for poor prognosis for non-small cell lung cancer (NSCLC). However, molecular mechanisms underlying the EPAS1 overexpression are not still fully understood. We explored a role of a single nucleotide polymorphism (SNP), rs13419896 located within intron 1 of the *EPAS1* gene in regulation of its expression. Bioinformatic analyses suggested that a region including the rs13419896 SNP plays a role in regulation of the *EPAS1* gene expression and the SNP alters the binding activity of transcription factors. *In vitro* analyses demonstrated that a fragment containing the SNP locus function as a regulatory region and that a fragment with *A* allele showed higher transactivation activity than one with *G*, especially in the presence of overexpressed c-Fos or c-Jun. Moreover, NSCLC patients with the *A* allele showed poorer prognosis than those with *G* at the SNP even after adjustment with various variables. In conclusion, the genetic polymorphism of the *EPAS1* gene may lead to variation of its gene expression levels to drive progression of the cancer and serve as a prognostic marker for NSCLC.

Introduction

Hypoxia-inducible factors (HIFs) are heterodimeric transcription factors that are members of the Per-ARNT-Sim (PAS) family. They are activated by a number of signaling inputs including

collection and analysis, decision to publish, or preparation of the manuscript.

Competing Interests: The authors have declared that no competing interests exist.

hypoxia, nutrient starvation, inflammation, oncogenic signals, mechanical stress, and in some cases, internal genetic polymorphisms [1–4]. The HIF transcription factors consist of alpha subunits (HIF-1α, HIF-2α, HIF-3α) that are regulated by the aforementioned signals while beta subunits known as aryl hydrocarbon receptor nuclear translocator (ARNT) are constitutively expressed and stimulate the transcription of more than a hundred target genes related to patho-physiological response [5, 6]. Among alpha subunits, HIF-1α and HIF-2α have been extensively studied. Although members of the alpha subunits share similarities in their structure, function and regulation *in vitro*, their roles *in vivo* are disparate during development and tumorigenesis [3, 5, 7].

The human HIF-2α gene known as endothelial PAS domain protein 1 (*EPAS1*), contains 16 exons and spans 90 kb on 2p21-p16. Expression of human HIF-2α has been identified in lung, carotid bodies, endothelial cells, glial cells, cardiomyocytes, renal fibroblasts and hepatocytes where it plays an important role in the regulation of oxygen physiology [3, 8]. This is of particular importance in the lung as it constitutes the site for oxygen exchange and provides the air-liquid interface for this purpose. HIF-2α proteins are expressed in type II pneumocytes and pulmonary endothelial cells in response to hypoxia as well as in epithelium and mesenchymal structures that give rise to the vascular endothelium [9, 10]. Furthermore, high levels of HIF-2α expression were linked to increased tumor size, invasion and angiogenesis in murine models of lung cancer [11,12]. Enhanced expression of HIF-2α protein in non-small cell lung cancer (NSCLC) tissue was reported to be a significant maker for poor prognosis [13–15].

Recently, it has been reported that several single nucleotide polymorphisms (SNPs) of *EPAS1* are associated with the development of osteoarthritis [16], retinopathy of prematurity [17], maximum metabolic performance in elite endurance athletes [18], physiologic adaptation in high altitude populations [19–22], and susceptibility towards renal cell carcinoma (RCC) and prostate cancer [23, 24]. However, the effects of these SNPs on expression levels of the *EPAS1* are scarcely understood.

Among these SNPs, we focused on Hap-tag SNPs of the *EPAS1* gene that may contribute to the adaptation to high-altitude hypoxia in Sherpas [22], considering lung as a target organ. Bioinformatic analyses prompted us to examine the role of rs13419896 SNP in regulation of the *EPAS1* gene expression and an association with prognosis of NSCLC.

Materials and Methods

Bioinformatic analyses

We interrogated transcription factor chromatin immunoprecipitation (ChIP-seq) datasets from the Encyclopedia of DNA Elements (ENCODE) consortium using the University of California, Santa Cruz (UCSC) Genome Browser (http://genome.ucsc.edu/ENCODE/) to find out candidate transcription factors that may bind on or in close proximity to the rs13419896 SNP site. Allele specific surveillance of transcription factors bound to the fragment containing the rs13419896 SNP was carried out using JASPAR CORE Vertebrata, an open-access database of matrix-based nucleotide profiles describing the binding preference of transcription factors [25].

DNA extraction and genotyping analysis

Genomic DNA was isolated from peripheral blood samples or frozen non-cancerous lung tissues as previously described [26, 27]. The following primer set was used to amplify a fragment including the SNP focus in *EPAS1* intron1; Forward: 5′ -CCTAATGAGCCTCTGGGAAAGTGC-3′ and Reverse: 5′ -CAATGGTGCCTCCTACCCTGTG-3′ . The PCR reaction conditions were 40 cycles of denaturation at 95°C for 30 sec, annealing at 63°C for 30 sec, and extension at 72°C for 30 sec. Sequencing of PCR products was carried out using the BigDye Terminator

Cycle Sequencing Kit and ABI PRISM 310 Genetic Analyzer automated sequencing system (Applied Biosystems, Foster City, CA, USA).

Cell lines and cell culture

Twenty-four human cancer cell lines consisting of a hepatoma cells HepG2, oral squamous cell carcinoma lines HSC-2, HSC-3, HSC-4, KB and KOSC2, breast cancers MCF-7, MDA-MB-231, MDA-MB-435S, MDA-MB-453, MDA-MB-468, BT-20, BT-474, SK-BR-3, T-47D, and ZR-75-1 and lung cancer cell lines A549, PC-6, PC-9, PC14, RERF-LC-Ad-1, RERF-LC-Ad-2, RERF-LC-KJ, and LC-S were obtained from ATCC (Manassas, VA) or JCRB (Osaka, Japan) between 2001 and 2007, and maintained in RPMI1640 or Dulbecco's modified Eagle's minimal essential medium (DMEM) (NACALAI TESQUE, Inc., Kyoto, Japan) containing 10% fetal bovine serum (FBS; BioWhittaker, Verviers, Belgium) as previously described [28–30]. *EPAS1* status of the cells was determined by sequencing analysis as described above.

RNA preparation and RT-PCR

Total RNA was prepared from frozen cell pellets using the QIAGEN RNeasy mini kit (QIAGEN, Inc., Valencia, CA) according to manufacturer instructions. Two micrograms of total RNA extracted from each cell line was reverse-transcribed using the High-Capacity cDNA Archive Kit (Applied Biosystems, Foster City, CA). A 1/200 dilution of the cDNA was subjected to real-time RT-PCR using TaqMan Gene Expression Assays (Applied Biosystems) for *EPAS1* and Pre-Developed TaqMan Assay Reagents (Applied Biosystems) for *ACTB* as housekeeping control. Three independent measurements were taken and averaged with relative gene expression levels calculated as ratios over *ACTB* expression for each cell line.

Immunoblot Analysis

To analyze protein expression, whole cell extracts were prepared from cultured cells with or without hypoxic treatment as previously described [30]. Fifty μg of protein was blotted onto nitrocellulose filters following SDS-polyacrylamide gel electrophoresis. Anti-EPAS1 (HIF-2α) (Cell Signaling Technology Japan, Tokyo) or anti-β-actin (sigma) was used as primary antibodies diluted as 1:500 or 1:5000. Anti-rabbit IgG or anti-mouse Ig horseradish peroxidase conjugate (Amersham Life Science) was used as a secondary antibody diluted as 1:2000 or 1:5000. Immunocomplexes were visualized using the enhanced chemiluminiscence reagent ECL Plus (Amersham Life Science).

Plasmid construction and luciferase reporter experiments

Annealed oligonucleotide fragments containing the *EPAS1* SNP locus rs13419896 (5′ -GGTACCAGTGTCTGAAAGTGAAGC**G**CTAGGATTGGTTACTGACGGTACC-3′ or 5′ -GGTACCAGTGTCTGAAAGTGAAGC**A**CTAGGATTGGTTACTGACGGTACC-3′) were subcloned into the *Kpn* I site of pGL4.26 (Promega, Madison, WI) with a minimal promoter driving the firefly luciferase reporter. C/EBP-β or c-MYC cDNA was amplified from total RNA of MCF-7 or HSC2 cells by RT-PCR and subcloned into pRc/CMV (Invitrogen, Carlsbad, CA) or pcDNA 3.1/V5-His-TOPO (Invitrogen). Constructs were confirmed by sequence analysis and designated as pGL4.26-EPAS1_G, pGL4.26-EPAS1_A, pCMV-C/EBP-β, or pcDNA-c-MYC, respectively. Rat c-Jun driven by the human β-actin promoter (c-Jun/β-actin) and human c-FOS expression vectors were generously provided by Dr. Masaharu Sakai (Hokkaido University) [31]. Transient transfections were performed where each pGL4.26-EPAS1 reporter construct (0.2 μg/15 mm well) with Renilla luciferase co-transfection control (pRL-SV40, 100 pg/

15-mm well) (Promega) was mixed with 0.4 μl of Trans-IT LT1 Transfection Reagent (TaKaRa, Japan) and added to the medium. In co-transfection experiments, 0.4 μg of pRc/CMV, c-Jun/β-actin, c-FOS, pcDNA-c-MYC or pCMV-C/EBP-β was mixed with EPAS1 reporters as above. Cells were incubated with the mixture for 24 h prior to quantification of luciferase reporter activity on the single-sample Mini Lumat LB 9505 luminometer (Berthold Technologies GmbH & Co. KG, Bad Wildbad, Germany) using the Dual Luciferase Assay Kit (Promega). *EPAS1* SNP reporter activity was calculated as ratios over Renilla luciferase activity and the average of three assays or more for each reporter was used for comparisons.

Patient studies

A total of 76 Japanese non-small cell lung cancer patients diagnosed at the Hiroshima University Hospital from 1991 to 1996 [4, 32] were enrolled in this study. Written informed consent was obtained from all individuals. This study was approved by the Institutional Genetic and Medical Ethics Committee at Hiroshima University. Patients and their clinicopathological characteristics of lung cancer were assessed according to the International Staging System for lung cancer [33], and are shown in Table 1. Briefly, a total of 76 lung cancer patients, whose average age was 65.8 (±8.2), consisted of 56 males and 20 female; 43 adenocarcinomas (AD), 29 squamous cell carcinomas (SCC), and 4 adeno-squamous cell carcinomas (ADSCC). Distribution of the lung cancer patients by stages (31 patients were at stage I, 7 at II, 25 at III and 13 at IV) is well matched to the broadly representative of the Japanese lung cancer population.

Statistical analysis

The primary outcomes in this study were lung cancer-specific mortality and risk of death. Survival time was calculated as the time from primary surgery to death due to lung cancer, censoring at the date of last contact or non-cancer death. Chi-square or Fisher's exact test was used to examine distributions of variables. Differences in survival were examined using log-rank test. Cox proportional hazard model was used to estimate the relative risk for death and 95% confidence intervals (CI). Statistical analyses were performed using a statistical software JMP version 10.0.2 (SAS Institute Inc., Cary, NC, USA), otherwise specified. Extended Fisher's exact test was conducted using "R": a language and environment for statistical computing (R Core

Table 1. Patient characteristics.

Patient demographics			
Total individual (%)		76 (100)	
Mean age (SD)		65.8	(8.2)
Gender (%)	Male	56 (73.7)	
	Female	20 (26.3)	
Differentiation[a]	Well	18 (25.0)	
	Moderate	35 (48.6)	
	Poor	19 (26.4)	
Stage[b]	I	31 (40.8)	
	II	7 (9.2)	
	III	25 (32.9)	
	IV	13 (17.1)	

[a]Differentiation was defined for NSCLC excluding four cases with adenosquamous cell carcinoma.
[b]Stage was assessed according to the International Staging System (Hermanek and Sobin, 1987).

doi:10.1371/journal.pone.0134496.t001